

HNPS Advances in Nuclear Physics

Vol 21 (2013)

HNPS2013



Analysis of the flow systematics in Au+Au collisions

M. Veselsky, Yu-Gang Ma, G. A. Souliotis

doi: [10.12681/hnps.2001](https://doi.org/10.12681/hnps.2001)

To cite this article:

Veselsky, M., Ma, Y.-G., & Souliotis, G. A. (2019). Analysis of the flow systematics in Au+Au collisions. *HNPS Advances in Nuclear Physics*, 21, 37–43. <https://doi.org/10.12681/hnps.2001>

Analysis of the flow systematics in Au+Au collisions

Martin Veselsky

Institute of Physics, Slovak Academy of Sciences, Dubravska cesta 9, 845 11 Bratislava, Slovakia

Yu-Gang Ma

Shanghai Institute of Applied Physics, Chinese Academy of Sciences, 2019 Jia-Luo Road, P.O. Box 800-204, Shanghai 201800, China

Georgios A. Souliotis

Laboratory of Physical Chemistry, Department of Chemistry, National and Kapodistrian University of Athens, and Hellenic Institute of Nuclear Physics, Athens 15771, Greece

Abstract

The new implementation of the Boltzmann-Uhling-Uhlenbeck equation, the VdWBUU simulation (with EoS-dependent in-medium nucleon-nucleon cross sections) appears to reproduce the flow observables in the Au+Au collisions in the energy range from 400 AMeV to 10 AGeV. The range of the feasible stiffness of the EoS can be identified, based on the analysis presented here, as encompassing compressibilities starting from 250 - 260 MeV and above, and thus consistent with the results of re-analysis of the giant monopole resonance data (250 - 310 MeV). Using that additional constraint, the range of feasible values of the stiffness of density dependence can be set as $\gamma = 1. - 1.25$, with the value $\gamma = 1$ appearing as a global value of stiffness of the symmetry energy feasible over the whole range of constrained compressibilities. The implementation of BUU with the free nucleon-nucleon cross sections can not describe correctly the global trends of flow observables.

1. Introduction

One of the main goals of intermediate-energy heavy-ion collisions (HIC) is to study properties of nuclear matter, especially to determine the nuclear equation of state (EoS). HIC provide a unique possibility to compress nuclear matter to a hot and dense phase within a laboratory environment. The pressures that result from the high densities achieved during such collisions strongly influence the motion of ejected matter and are sensitive to the EoS. With the hard work of the researchers over the last three decades, the EoS of symmetric nuclear matter was studied in detail by the study of giant resonances, collective flow as well as multifragmentation [1–4]. The study of the EoS of isospin asymmetric nuclear matter is currently underway, particularly, for the density dependence of symmetry energy. Considerable progress has been made in determining the sub- and supra-saturation density behavior of the symmetry energy [5–12]. The latter issue is still an unanswered question in spite of recent findings in term of neutron-proton elliptic flow ratio and difference [10, 11]. However, the former topic is understood to some extent [5–8], although, more efforts are needed for precise measurements.

Email addresses: martin.veselsky@savba.sk (Martin Veselsky), ygma@sinap.ac.cn (Yu-Gang Ma), soulioti@chem.uoa.gr (Georgios A. Souliotis)

2. Boltzmann-Uehling-Uhlenbeck equation with EoS-dependent in-medium nucleon-nucleon cross sections

A transport model is very useful to treat heavy ion collision dynamics and obtain important information of nuclear matter EoS as well as the symmetry energy. In intermediate energy heavy ion collisions, the Boltzmann-Uehling-Uhlenbeck (BUU) model is an extensively useful tool [13, 14], which takes both Pauli blocking and mean field into consideration. The BUU equation reads

$$\begin{aligned} \frac{\partial f}{\partial t} + v \cdot \nabla_r f - \nabla_r U \cdot \nabla_p f &= \frac{4}{(2\pi)^3} \int d^3 p_2 d^3 p_3 d\Omega \\ \frac{d\sigma_{NN}}{d\Omega} v_{12} \times [f_3 f_4 (1-f)(1-f_2) - f f_2 (1-f_3)(1-f_4)] \\ \delta^3(p + p_2 - p_3 - p_4), \end{aligned} \quad (1)$$

where $f=f(r, p, t)$ is the phase-space distribution function. It is solved with the test particle method of Wong [15], with the collision term as introduced by Cugnon, Mizutani and Vandermeulen [16]. In Eq.(1), $\frac{d\sigma_{NN}}{d\Omega}$ and v_{12} are in-medium nucleon-nucleon cross section and relative velocity for the colliding nucleons, respectively, and U is the single-particle mean field potential with the addition of the isospin-dependent symmetry energy term, which in its simplest form is usually expressed as

$$U = a\rho + b\rho^\kappa + 2a_s\left(\frac{\rho}{\rho_0}\right)^\gamma \tau_z I, \quad (2)$$

where $I = (\rho_n - \rho_p)/\rho$, ρ_0 is the normal nuclear matter density; ρ , ρ_n , and ρ_p are the nucleon, neutron and proton densities, respectively; τ_z assumes value 1 for neutron and -1 for proton, coefficients a , b and κ represent properties of the symmetric nuclear matter while the last term describes the density dependence of the symmetry energy, with a_s representing the symmetry energy coefficient and γ determining the density dependence.

When considering influence of the symmetry energy on emission rates of nucleons in nucleus-nucleus collisions, one needs to understand whether and how the medium represented by the equation of state can influence relative probabilities of emission of protons and neutrons. Theoretical investigations of the density-dependence of in-medium nucleon-nucleon cross section were carried out for symmetric nuclear matter [17, 18], and significant influence of nuclear density on resulting in-medium cross sections was observed in their density, angular and energy dependencies. Using momentum-dependent interaction, ratios of in-medium to free nucleon-nucleon cross sections were evaluated via reduced nucleonic masses [19] and used for transport simulations. Still, transport simulation are mostly performed using parametrizations of the free nucleon-nucleon cross sections, eventually scaling them down empirically or using simple prescriptions for density-dependence of the scaling factor [20]. In the recent work [21], a prescription for estimation of the density-dependence of the in-medium nucleon-nucleon cross sections corresponding to the specific form of phenomenological nuclear equation of state was presented. Such possibility to establish a simple dependence of nucleon-nucleon cross sections on density, temperature and symmetry energy is potentially important for a wide range of problems in nuclear physics and astrophysics.

As demonstrated in [21], in order to find a relation between the equation of state and in-medium nucleon-nucleon cross sections one can turn attention specifically to the Van der Waals equation of state. To proceed in this direction, the equation of state of nuclear matter can be formulated as an expression for the pressure which can be in general written as

$$p = \left\langle \frac{f_{5/2}(z)}{f_{3/2}(z)} \right\rangle \rho T + a\rho^2 + p_{pot}(\rho, T, I) + p_{kin}(\rho, T, I) \quad (3)$$

where $p_{pot}(\rho, T, I)$ represents the component of pressure related to single particle potential (with the exception of the pressure term $a\rho^2$ which is treated separately) and $p_{kin}(\rho, T, I)$ is caused by the kinetic term of the symmetry energy. The Fermi integrals $f_{5/2}(z)$, $f_{3/2}(z)$ reflect the Fermionic nature of nucleons.

It is then possible to formally transform the above equations of state (and practically any other equation of state) into the form analogous to the Van der Waals equation. Then corresponding expression for the proper volume in the Van der Waals form will be

$$b' = \frac{1}{\rho} \frac{p_{pot}(\rho, T, I) + p_{kin}(\rho, T, I)}{\langle \frac{f_{5/2}(z)}{f_{3/2}(z)} \rangle \rho T + p_{pot}(\rho, T, I) + p_{kin}(\rho, T, I)} \quad (4)$$

which demonstrates immediately that for any form of equation of state it always exhibits a $1/\rho$ -dependence at zero temperature. The expression $\langle \frac{f_{5/2}(z)}{f_{3/2}(z)} \rangle T$ is a classical temperature which can be estimated easily from the momentum distribution of nucleons.

3. Analysis of the flow observables

The flow observables were introduced primarily as observables directly related to the equation of the state of nuclear matter. Essentially, different flow observables can be identified with the coefficients of the Fourier expansion of the azimuthal angular distribution relative to the reaction plane.

Flow observable, related to the first Fourier coefficient v_1 is usually called as directed flow. It can be alternatively expressed in terms of a slope of the momentum p_x (in the reaction plane) at mid rapidity. The systematics of this observable for protons observed in the semi-peripheral collisions ($b=5.5-7.5$ fm) of Au+Au at various beam energies was published in [22] and it exhibits an initial linear rise from zero to the maximum value of about 0.37 GeV/c at beam energy 400 AMeV, followed by linear decrease to the value 0.1 at 10 AGeV. The positive values of the slope appear to signal that the stopping in the nuclear medium is not full and the effect of the attractive mean-field is stronger than stopping due to two-body nucleon-nucleon collisions. The elliptic flow is characterized by the value of the second Fourier coefficient v_2 and its systematics for the protons observed in the semi-peripheral collisions of Au+Au at mid-rapidity was published in the work [23]. Below 100 AMeV the elliptic flow is positive, reflecting the binary dissipative nature of the semi-peripheral collision at such beam energies, reflected in mostly in-plane proton emission. Furthermore, at approximately 150 AMeV the elliptic flow assumes negative value, reflecting the squeeze-out effect where the protons from the participant zone are emitted predominantly in the out-of plane direction. When combined, these two systematics provide a good set of experimental data for testing of the transport codes and for determination of the parameters of the equation of the state of nuclear matter.

A new variant of the transport code for simulation of the nucleus-nucleus collisions, introduced in the work [21], was used for analysis of flow observables. At variance to previous codes used for the solution of the Boltzmann-Uhling-Uhlenbeck equation (BUU), the nucleon-nucleon cross sections used for evaluation of the collision term, are estimated directly from the equation of state used for evaluation of the mean-field potential using the formula (4). The whole calculation is based on the selected equation of state and there is no need to use free or empirically estimated in-medium cross sections. These simulations will be described using the acronym VdWBUU, while the reference simulations using the free nucleon-nucleon cross sections of Cugnon [16] will be described as fBUU. The particles are considered as emitted when they are separated in the phase-space from any other particle and separation is large enough to assure that two particles are not part of a cluster (a condition $\Delta\vec{p}\Delta\vec{r} > 2h$ is implemented).

The equations of state used in many preceding works are typically two types of the mean field, the soft EoS with the compressibility K of 200 MeV (corresponding to the value $\kappa = 7/6$ in the equation (2)), and the hard EoS with K of 380 MeV ($\kappa = 2$), as first introduced in the work [13]. These two equations of the state can be considered as two extremes and many intermediate equations of the state are feasible, with the compressibility K depending linearly on κ , as shown in the equation

$$K = 9\kappa(B + \frac{\epsilon_F(\rho_0)}{5}) - \frac{6}{5}\epsilon_F(\rho_0) \quad (5)$$

where B is the binding energy at saturation density (with typically assumed value $B = 16$ MeV) and $\epsilon_F(\rho_0)$ is the Fermi energy at the saturation density ρ_0 (typically set to $\rho_0 = 0.16 \text{ fm}^{-3}$). In the present work, the intermediate values of $\kappa = 4/3, 3/2, 5/3$ were used.

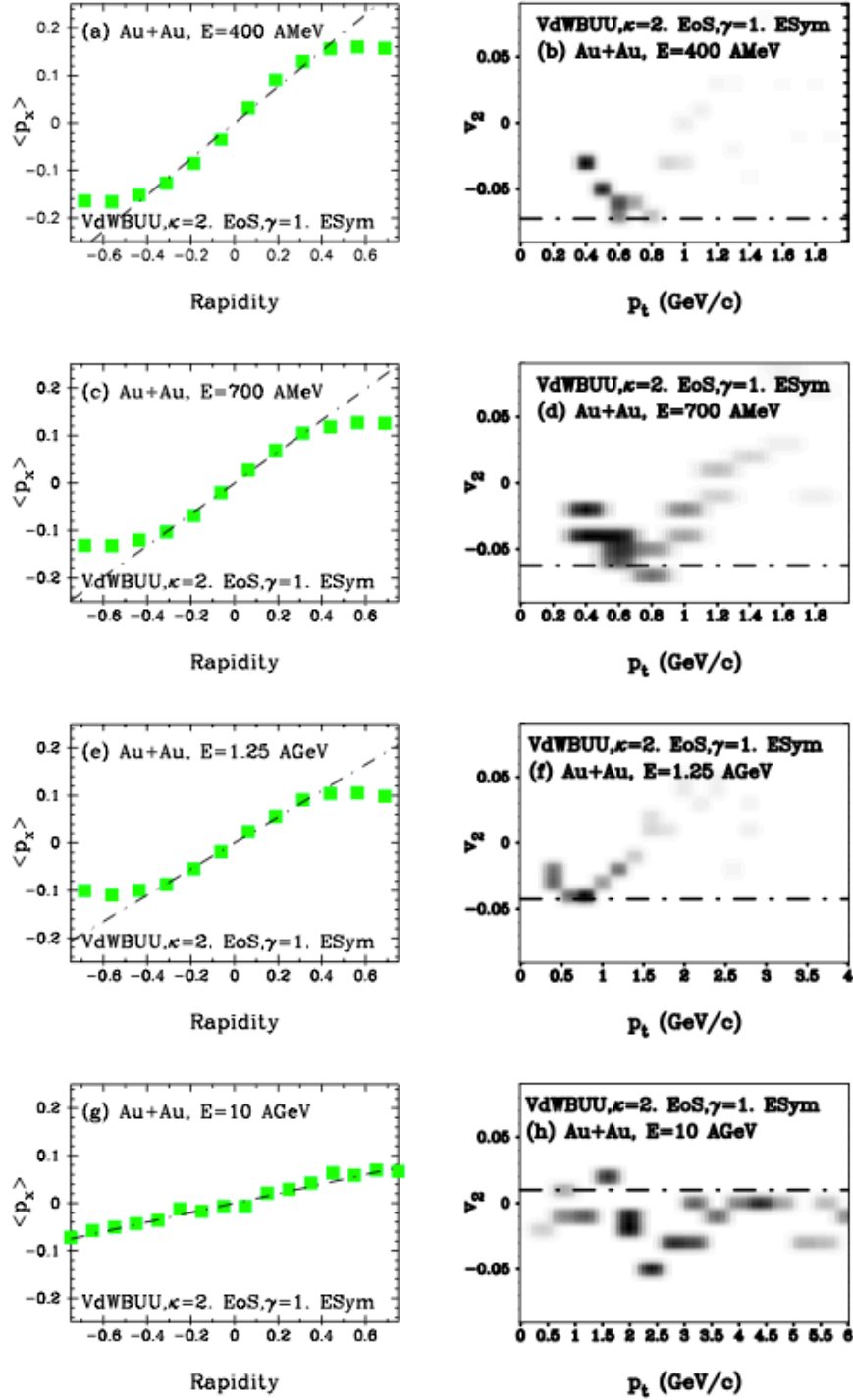


Figure 1: Systematics of the proton directed flow (left panels, lines show experimentally observed slopes) and the transverse momentum dependence of the calculated proton elliptic flow at mid-rapidity versus the experimental value (boxes and the dash-dotted lines in right panels, respectively) in the collisions of Au+Au at beam energies ranging from 400 AMeV to 10 AGeV. Results were obtained using the VdWBUU simulation using the stiff EoS with $\kappa = 2$ and the symmetry energy potential parametrization with $\gamma = 1$.

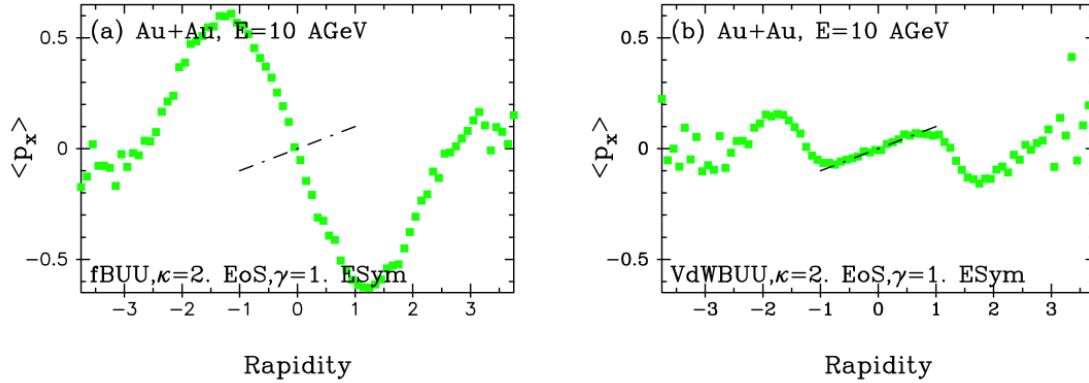


Figure 2: Proton directed flow in the collisions of Au+Au at beam energy of 10 AGeV. Results were obtained using the simulation with and without EoS-dependent in-medium nucleon-nucleon cross sections (left and right panels, respectively) using the stiff EoS with $\kappa = 2$ and the symmetry energy potential parametrization with $\gamma = 1$. Lines show experimentally observed slope.

The density dependence of the symmetry energy is parameterized in a way that the symmetry energy term, corresponding to the potential term of the type, shown in equation (2), is complemented by an analogous term with $\gamma_k = 2/3$, representing the kinetic energy of the degenerate Fermi gas at zero temperature (with the corresponding coefficient assumed to be related to the Fermi energy as $a_k = \epsilon_F(\rho_0)/3$). In the present work, the density dependences of the symmetry potential ranging from the asy-soft ($\gamma = 1/2$) to asy-stiff ($\gamma = 2$) were used ($\gamma = 4/5, 1, 5/4, 3/2$ being the intermediate values). The relative weight of the two terms was set to keep the value of the symmetry energy coefficient at normal nuclear density at the value of 32 MeV.

As one of the viable variants of the calculations appears to be the VdWBUU simulation (with in-medium nucleon-nucleon cross sections) using the stiff EoS and the symmetry energy potential parametrization with $\gamma = 1$. Besides the selection criterion mentioned above, the low energy cutoff was set at transverse momentum 0.4 GeV/c, since low-energy particles below such cutoff represent essentially the initial transverse momenta randomly generated according to the zero temperature Fermionic momentum distribution. Furthermore, also the effect of Coulomb interaction, which affects primarily such low-energy particles, is not taken into account in the BUU. The results are shown in the Figure 1. As one can see the measured directed flow is reproduced well over the whole range of beam energy and thus over a range of the maximum densities of nuclear matter achieved in collisions. The maxima of the negative elliptic flow shown in the right panels reach the experimentally observed value.

To understand better the dramatic effect of the EoS-dependent in-medium nucleon-nucleon cross sections on directed flow, the results for the beam energy 10 AGeV with and without EoS-dependent in-medium nucleon-nucleon cross sections are compared in Figure 2 (the free nucleon-nucleon cross sections being used in the latter case). It is noteworthy that the free nucleon-nucleon cross sections lead to much stronger stopping and thus negative value of directed flow, while their reduction caused by density dependence leads to reproduction of the measured value and thus correct description of dynamics in the participant zone leading to splash behavior.

The results of the analysis are summarized in the Figure 3. The filled triangular area in the γ vs K_0 plot shows the combinations of the EoS and symmetry energy parameterizations, which either lead to reasonable agreement or can not be conclusively ruled out as feasible for the description of properties of nuclear matter. The effect of stiffening of the EoS appears to lead to weakening of the effect of density dependence of the symmetry energy. It appears that the density dependence with $\gamma = 1$ can be identified as a globally feasible value of the stiffness of the symmetry energy. The range of the possible stiffness of the EoS can be identified, based on the analysis presented here, as encompassing compressibilities starting from 250 - 260 MeV and

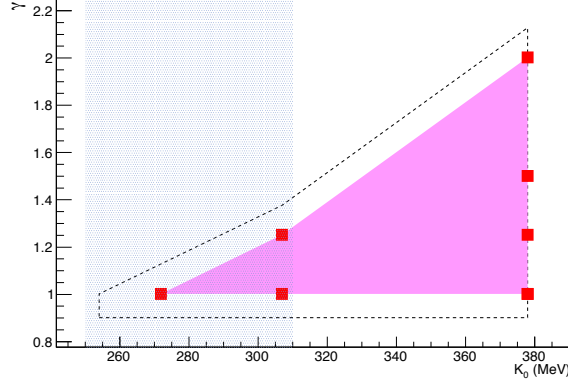


Figure 3: The filled area in the γ vs K_0 plot shows the values of the EoS and symmetry energy parameters, constrained by the analysis using the VdWBUU simulations (squares show the values where calculation was performed and dashed line shows the uncertainty resulting from restricted set of calculated points). Dotted area shows the constrained values of K_0 from re-analysis of giant monopole resonance data [24].

above. Remarkably, this range is consistent with the results of recent re-analysis of the data from giant monopole resonance [24], where the range of $K_0 = 250 - 310$ MeV (shown as dotted area in Figure 3) was determined after modification of the fitting procedure, used to determine compressibility, thus correcting the earlier constrained softer values between 200 - 240 MeV. When combining our results with results of the work [24], it is possible to further constrain the values of γ , which can be restricted to range $\gamma = 1. - 1.25$, with the most probable value around $\gamma = 1$. The resulting values appear to be in agreement with results of earlier studies of nucleus-nucleus collisions [10, 19]. Furthermore, the range of feasible compressibilities are strongly correlated to the results of astrophysical evaluations of the radius of neutron stars. The values of $E_{sym}(\rho_0)$ and L constrained using radii of neutron stars depend rather weakly on the compressibility of the EoS [25] and thus relatively stiffer equations of state appear appropriate, even if restrictions due to causality must be considered. Also, the recent re-analysis of the determination of the neutron star radii appears to lead to larger radii with lower limit around 14 km [26] and thus to favor stiffer equation of the state. Furthermore, also the relatively thick neutron skin of ^{208}Pb , reported by the PREX experiment [27, 28], appears to favor a stiffer equation of state [29].

4. Conclusions

In summary, the new implementation of the BUU, the VdWBUU simulation (with EoS-dependent in-medium nucleon-nucleon cross sections) appears to reproduce the flow observables in the Au+Au collisions in the energy range from 400 A MeV to 10 A GeV. The range of the feasible stiffness of the EoS can be identified, based on the analysis presented here, as encompassing compressibilities starting from 250 - 260 MeV and above, and thus consistent with the results of re-analysis of the giant monopole resonance data (250 - 310 MeV). Using that additional constraint, the range of feasible values of the stiffness of density dependence can be set as $\gamma = 1. - 1.25$, with the value $\gamma = 1$ appearing as a global value of stiffness of the symmetry energy feasible over the whole range of constrained compressibilities. The implementation of BUU with the free nucleon-nucleon cross sections can not describe correctly the global trends of flow observables.

Acknowledgments

This work is supported by the Slovak Scientific Grant Agency under contracts 2/0105/11 and 2/0121/14, by the Slovak Research and Development Agency under contract APVV-0177-11, by the NSFC of China

under contract Nos. 11035009, 10979074, the Knowledge Innovation Project of CAS under Grant No. KJCX2-EW-N01 (Y.G.M.).

References

- [1] D. H. Youngblood, H. L. Clark, and Y.-W. Lui, Phys. Rev. Lett. **82**, 691 (1999). 06).
- [2] J. B. Natowitz *et al.*, g, Phys. Rev. Lett. **89**, 212701 (2002).
- [3] P. Danielewicz, R. Lacey, and W. G. Lynch, Science **298**, 1592 (2002).
- [4] W. Reisdorf *et al.*, Nucl. Phys. A **876**, 1 (2012).
- [5] M. B. Tsang *et al.*, Phys. Rev. Lett. **92**, 062701 (2004).
- [6] M. A. Famiano *et al.*, Phys. Rev. Lett. **97**, 052701 (2006).
- [7] M. B. Tsang *et al.*, Phys. Rev. Lett. **102**, 122701 (2009).
- [8] S. Kumar *et al.*, Phys. Rev. C **84**, 044620 (2011).
- [9] B. A. Li, L. W. Chen, and C. M. Ko, Phys. Rep. **464**, 113 (2008). (2009).
- [10] P. Russotto *et al.*, Phys. Lett. B **697**, 471 (2011).
- [11] M. D. Cozma, Phys. Lett. B **700**, 139 (2011).
- [12] S. Gautam *et al.*, Phys. Rev. C **83**, 034606 (2011).
- [13] G. F. Bertsch, H. Kruse, and S. Das Gupta, Phys. Rev. C **29**, 673 (1984).
- [14] H. Kruse, B. V. Jacak, and H. Stöcker, Phys. Rev. Lett. **54**, 289 (1985).
- [15] C. Y. Wong, Phys. Rev. C **25**, 1460 (1982).
- [16] J. Cugnon, T. Mizutani, and J. Vandermeulen, Nucl. Phys. A **352**, 505 (1981).
- [17] G. Q. Li, and R. Machleidt, Phys. Rev. C **48**, 1702 (1993); Phys. Rev. C **49**, 566 (1994).
- [18] T. Alm, G. Ropke, and M. Schmidt, Phys. Rev. C **50**, 31 (1994); T. Alm, G. Ropke, W. Bauer, F. Daffin, and M. Schmidt, Nucl. Phys. A **587**, 815 (1995).
- [19] B. A. Li, and L. W. Chen, Phys. Rev. C **72**, 064611 (2005).
- [20] D. Klakow, G. Welke, and W. Bauer, Phys. Rev. C **48**, 1982 (1993).
- [21] M. Veselsky, Y.G. Ma, Phys. Rev. C **87** (2013) 034615.
- [22] N. Herrmann, J. P. Wessels, and T. Wienold, Ann. Rev. Nucl. Part. Sci. **49** (1999) 581.
- [23] A. Andronic, J. Lukasik, W. Reisdorf, and W. Trautmann, Eur. Phys. J. **30** (2006) 31.
- [24] J.R. Stone, N.J. Stone and S.A. Moszkowski, arXiv:1404.0744 [nucl-th].
- [25] K. Hebeler, J.M. Lattimer, C.J. Pethick and A. Schwenk, arXiv:1303.4662 [astro-ph.SR].
- [26] V. Suleimanov, J. Poutanen, M. Revnivtsev and K. Werner, Astrophys. J. **742** (2011) 122.
- [27] S. Abrahamyan *et al.*, Phys. Rev. Lett. **108**, 112502 (2012).
- [28] C. Horowitz *et al.*, Phys. Rev. C **85**, 032501 (2012).
- [29] F.J. Fattoyev and J. Piekarewicz, arXiv:1306.6034 [nucl-th].